A thick symmetrical aerofoil oscillating about zero incidence angle

S. Raghunathan and O. O. Ombaka*

Experimental investigations on a NACA 0018 aerofoil oscillating about mean incidence angle of 0° with amplitude of 16° are described. The results show an increase in incidence angle at which stall occurs, in maximum lift coefficient, and in the extent of hysteresis loop, with increase in reduced frequency.

Keywords: *aerofoils, airflow oscillation, Wells turbine, fluid flow*

The principle of operation and performance of the Wells self-rectifying air turbine for wave energy application has been described in several reports (see for example Ref 1). The frequencies of airflow oscillations in an oscillating water-column wave-energy device are generally less than 1 Hz; and the prediction methods, both theoretical and experimental, assume that the effect of such low frequency airflow oscillations on the performance of the Wells turbine can be neglected.

However, recent tests on a Wells turbine in an oscillating airflow rig at low frequencies[2] have shown that the above assumption is questionable and, for an accurate prediction of the turbine performance, a better understanding of the behaviour at low air flow frequencies of the thick symmetrical aerofoil blades is necessary.

There are several reports[3-8] on the aerodynamics of oscillating aerofoils, in particular on the dynamic stall associated with the oscillations. It is understood that the dynamic stall is sensitive to aerofoil geometry and mean incidence angle, the amplitude and frequency of oscillations, and the free stream conditions. High frequency oscillations about a mean incidence angle close to that for static stall, postpone the stall and also produce an increase in lift.

The above investigations were generally limited to thin aerofoils and at incidence angles close to that for static stall. In the case of the Wells turbine the oscillations of airflow occur at a mean incidence angle of zero, and the aerofoils are relatively thicker. This paper presents experimental investigations on a NACA 0018 aerofoil oscillating about mean incidence angle of zero, at reduced frequency range 0 to 5.88×10^{-3} and amplitude of $\pm 16°$.

The experimental details

The experiments were conducted in a 0.84 m × 1.145 m low speed tunnel. The turbulence level in the tunnel was 0.2%. The model was a NACA 0018 aerofoil, 0.15 m chord and 0.36 m span with end plates and mounted horizontally in the tunnel (Figs 1 and 2). The aerofoil was made of three spanwise sections. The middle section had 28 pressure orifices as shown in Fig 1. The oscillating drive mechanism consisted of a crank, connecting rod, flywheel and a pulley and belt system attached to a variable speed motor. The connecting rod was set to produce a mean incidence angle of zero. The amplitude of the oscillations, calibrated in degrees, was fixed by attaching the rod to a specific radial location on the flywheel. The measurements included pressure distribution for varying incidence angle, pressure as a function of time for various locations and incidence angle as a function of time. The pressure measurements were made by pressure transducers type FC040 located at the end of 1 m long tubes from the pressure orifice. It has been shown[9] that for a frequency range 0 to 4 Hz, the effect of tubing on the pressure attenuation is negligible up to a length of 1.5 m. A potentiometer was used to measure the incidence angle. The data were recorded on a X-Y recorder.

All the tests were performed at a free stream velocity of 24 m s^{-1} which corresponds to a Reynolds number based on the chord of 2.4×10^5. The test frequencies were 0 Hz (static tests), 2.5 Hz and 1.0 Hz. The angle of incidence was in the range $\pm 16°$.

Results and discussion

The pressure distributions from the static tests ($S_t = 0$) on the NACA 0018 aerofoil for various incidence angles are shown in Fig 3. The blade chord Reynolds number for these tests was 2.4×10^5. The pressure distributions are typical for a thick symmetrical aerofoil, with the separation on the surface propagating upstream with the increase in incidence angle. On the upper surface, at an incidence angle of 14°, the flow appears to have separated for $x/c \gtrsim 0.3$; whereas, at an incidence of 16°, the separation is complete.

Figs 4a and 4b show typical pressure-time histories at various chordwise locations for the aerofoil oscillating in the range $\pm 16°$ incidence angle. The blade chord Reynolds number and reduced frequency for these tests were 2.4×10^5 and 1.56×10^{-3}, respectively. The figures also show the incidence angle of the aerofoil as a function of time. On these graphs the incidence angle variations are marked as follows:

A to B 0 to 16°

B to C 16° to 0°

C to D 0° to −16°

D to A −16° to 0°

* Department of Aeronautical Engineering, Queen's University of Belfast, Belfast, N. Ireland, UK

Received 6 March 1985 and accepted for publication on 11 June 1985

If the curve ABCDA is split into two components ABC and CDA, the curve ABC corresponds to the upper surface of the aeorfoil for the incidence angles 0° to 16° to 0° whereas the curve CDA corresponds to the lower surface of the aerofoil for the incidence angles 0° to −16° to 0°, which is the reason for these two halves of the curve being not exactly identical. It is observed that at $x/c=0.0$ the value of C_P is maximum and is equal to unity at 0° incidence as expected. The value of C_P is minimum at ±16° incidence. The difference in C_P values between +16° and −16° can be attributed to the sensitivity of leading edge pressure to the exact location of the pressure hole and any minor imperfections in the symmetry of the leading edge. At $x/c=0.025$ the C_P value at $\alpha=+16°$ (point B) is high and negative as this represents the upper surface at high incidence angles. In principle the value of C_P at $\alpha=-16°$, which is positive (point D), would be the same as that on the lower surface at the same chordwise location at $\alpha=+16°$. The change in C_P values with incidence angle reduces towards the trailing edge, as seen from the plots at $x/c=0.3$, 0.5, 0.7 and 1.0. It is seen from these traces that the flow appears to separate on the upper surface for $\alpha \gtrsim +14°$ at $x/c=0.15$ and $\alpha > +10°$ at $x/c=0.7$, indicating the forward movement of separation with the increase in incidence angle. The unsteady pressures in the separated flow can also be observed from these traces, although the transducer responded only to low frequencies. These unsteady pressures are also

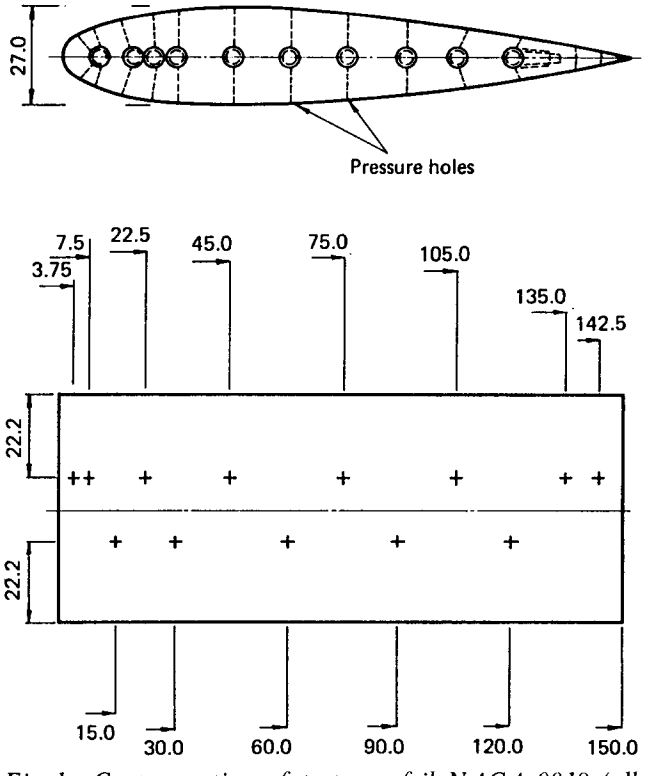

Fig 1 Centre section of test aerofoil NACA 0018 (all dimensions in mm)

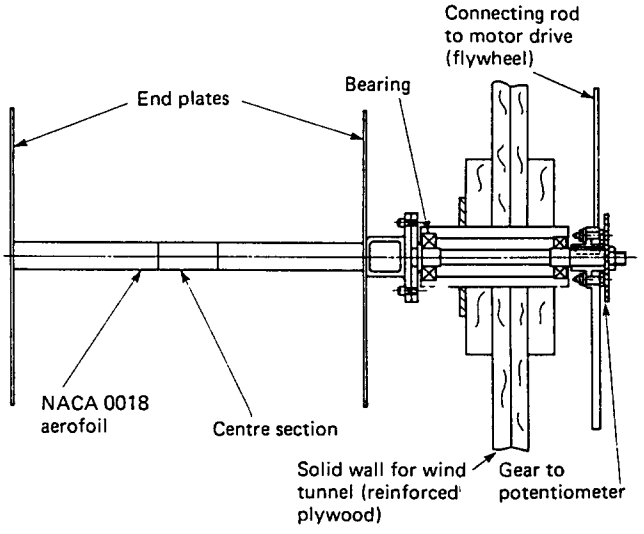

Fig 2 Model arrangement in tunnel

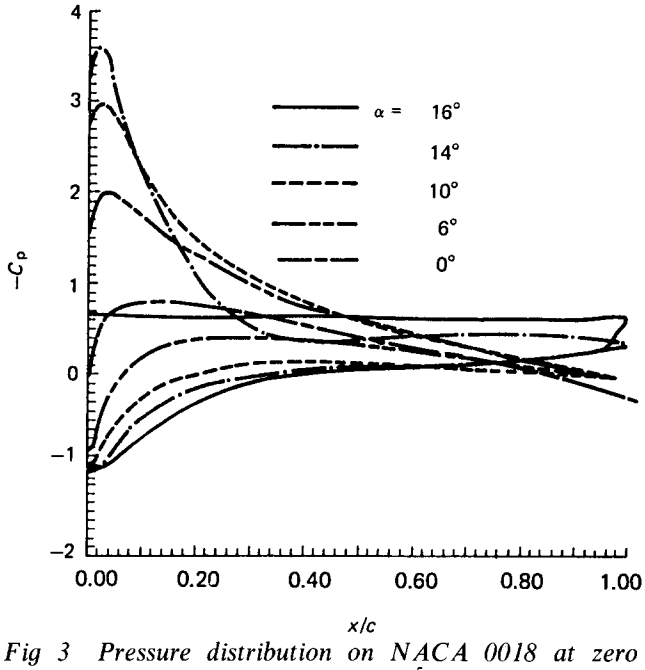

Fig 3 Pressure distribution on NACA 0018 at zero frequency; $S_t=0.00000$, $Re=2.4\times10^5$

Notation

c	Chord length
C_L, C_D	Lift and drag coefficients, respectively
C_L^*, C_D^*	Ratio of oscillating values of lift and drag coefficients, respectively to the corresponding static values, C_L/C_{L0}, C_D/C_{D0}
C_P	Pressure coefficient, $(P-P_\infty)/q_\infty$
f	Angular frequency
P, P_∞	Local and free stream static pressures, respectively
q_∞	Dynamic pressure, $\frac{1}{2}\rho V_\infty^2$
Re	Reynolds number, $V_\infty C/\nu$
S_t	Reduced frequency, fC/V_∞
t	Time
V_∞	Free stream velocity
x/c	Chordwise distance from leading edge
ρ	Density of air
ν	Kinematic viscosity of air
α	Incidence angle, $\alpha_m+\alpha_0 \sin 2\pi ft$
α_m	Mean incidence angle
α_0	Amplitude of oscillation
$\dot{\alpha}$	Rate of increase of incidence angle

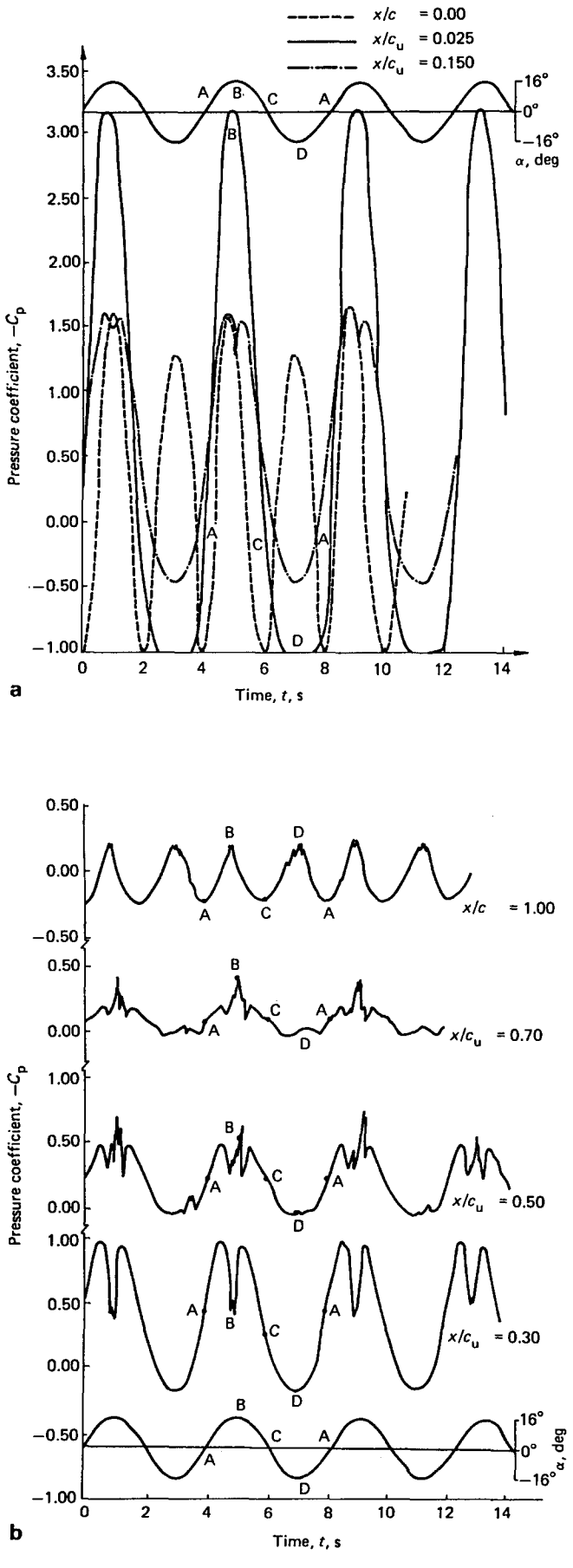

Fig 4 Pressure-time histories; $S_t = 1.56 \times 10^{-3}$, $Re = 2.4 \times 10^5$

communicated to the lower surface as can be seen from the results on the lower surface (point D) at $x/c = 0.7$.

The pressure distributions at incidence angles of 0°, 6°, 10°, 14° and 16° from steady measurements are compared with the corresponding results from the oscillating aerofoil tests in Figs 5 to 9. The oscillating aerofoil tests shown here correspond to $S_t = 5.88 \times 10^{-3}$.

Referring to Fig 5 it is observed that there is a reduction in the magnitude of the minimum C_p with the oscillating aerofoil when compared with the static test

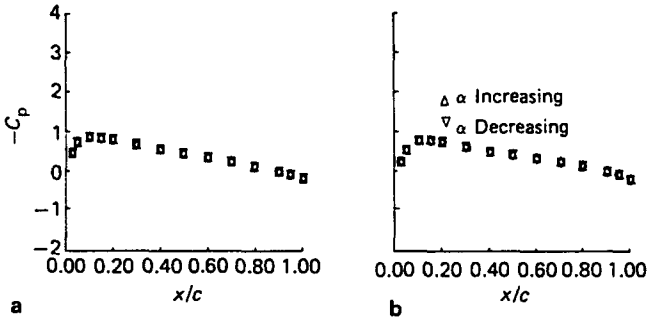

Fig 5 Pressure distribution at $\alpha = 0°$: *(a)* $S_t = 0.00000$; *(b)* $S_t = 5.88 \times 10^{-3}$

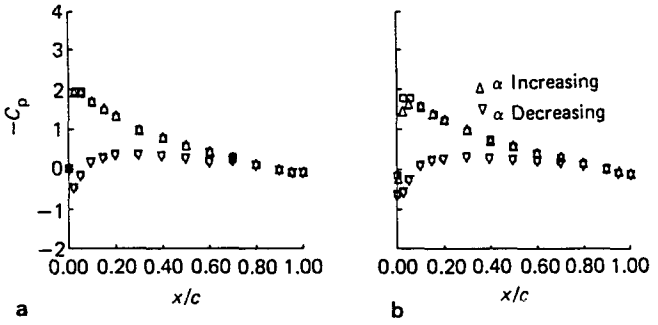

Fig 6 Pressure distribution at $\alpha = 6°$: *(a)* $\alpha = 6.0°$, $S_t = 0.00000$; *(b)* $\alpha = 6.4°$, $S_t = 5.88 \times 10^{-3}$

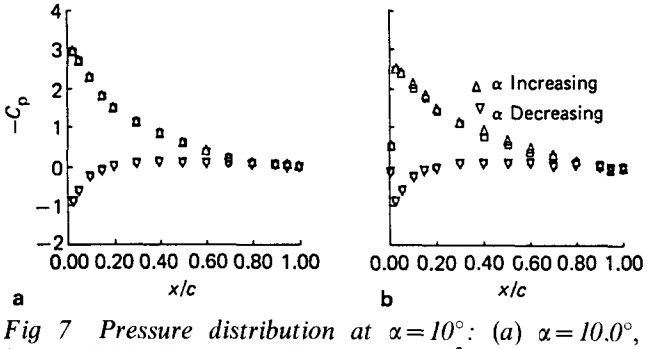

Fig 7 Pressure distribution at $\alpha = 10°$: *(a)* $\alpha = 10.0°$, $S_t = 0.00000$; *(b)* $\alpha = 9.6°$, $S_t = 5.88 \times 10^{-3}$

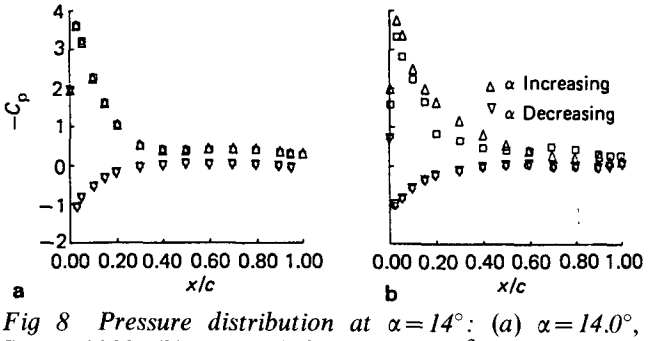

Fig 8 Pressure distribution at $\alpha = 14°$: *(a)* $\alpha = 14.0°$, $S_t = 0.00000$; *(b)* $\alpha = 14.4°$, $S_t = 5.88 \times 10^{-3}$

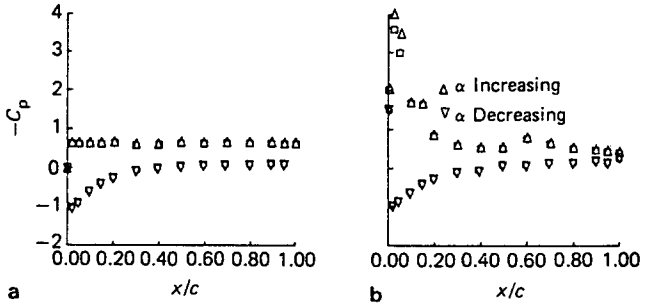

Fig 9 Pressure distribution at $\alpha = 16.0°$: (a) $S_t = 0.00000$; (b) $S_t = 5.88 \times 10^{-3}$

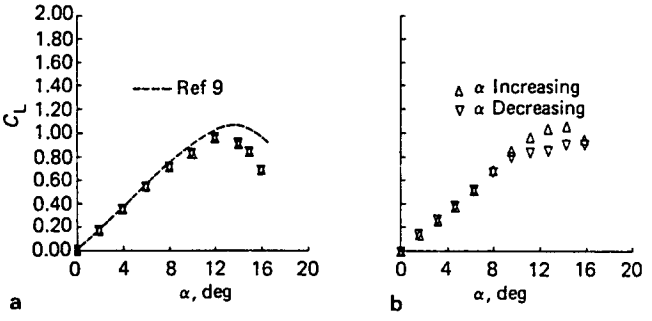

Fig 10 Effect of frequency on C_L: (a) $S_t = 0.00000$; (b) $S_t = 5.88 \times 10^{-3}$

results. The position where minimum C_P occurs is not sensitive to the frequency of oscillations.

At $\alpha = 6°$, the effect of oscillating the aerofoil is to move the position of minimum C_P slightly downstream. The pressure distribution on the lower surface has remained invariant with the frequency.

Noticeable changes between $S_t = 0$ and $S_t = 5.88 \times 10^{-3}$ begin to appear on the upper surface at $\alpha = 10°$. For $S_t = 5.88 \times 10^{-3}$ C_P values for increasing incidence angle are slightly higher than corresponding values for decreasing incidence angle. This is known as the hysteresis is effect and is due to the viscous effects and local velocity variation with time. There is a sign of separation at the trailing edge for both values of $S_t = 0$ and $S_t = 5.88 \times 10^{-3}$.

The hysteresis effects at $S_t = 5.88 \times 10^{-3}$ are more pronounced at $\alpha = 14.0°$ where the point of flow separation is at $x/c = 0.5$ for the increasing incidence and at $x/c = 0.4$ for the decreasing incidence, in comparison with $x/c = 0.3$ for $S_t = 0$. Therefore the extent of flow separation is generally reduced under dynamic conditions.

The incidence angle of 16° corresponds to a complete separation on the suction surface for the static aerofoil. This is not the case for the oscillating aerofoil, for which the flow on the suction surface is still attached up to $x/c = 0.3$. For the aerofoil oscillating in the range $+16°$ to $-16°$, the incidence angle of 16° occurs at the same instant of time for both the increasing and decreasing incidence angle.

Figs 10 and 11 show the variation of C_L and C_D, determined from pressure measurements, with incidence angle for $S_t = 0$ and $S_t = 5.88 \times 10^{-3}$. The result of a static test on NACA 0018 profile at a Reynolds number $Re = 3.3 \times 10^5$ from Ref 10 is also shown for comparison. Referring to Fig 10 the static tests results agree closely with that of Ref 10 until the stall. The present experiments at a lower Reynolds number show an earlier stall of $\alpha_{stall} = 12°$ and maximum value of $C_L = 0.97$. The hysteresis effect can be clearly seen at $S_t = 5.88 \times 10^{-3}$. The maximum value of C_L and the stall angle with increasing incidence angle are 0.99 and 14°, respectively.

The results agree with the general theory of dynamic stall which indicates that the aerodynamic forces on a two-dimensional aerofoil during large amplitude pitching motion are dominated by intense vorticity shed from the vicinity of the leading edge of the aerofoil, resulting in postponement of stall angle and an increase in maximum lift. Ref 6 also shows similar results with the increase in reduced frequency.

The C_D versus α curves shown in Fig 11 also show a postponement of stall. For $S_t = 0$, there is a gradual increase in C_D until $\alpha = 12°$, beyond which C_D increases rapidly. At $S_t = 5.88 \times 10^{-3}$, the rapid increase in the drag

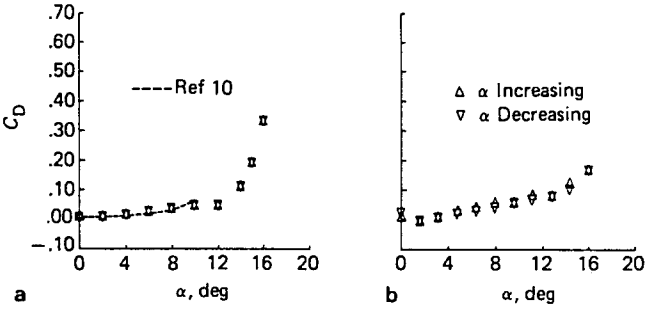

Fig 11 Effect of frequency on C_D: (a) $S_t = 0.00000$; (b) $S_t = 5.88 \times 10^{-3}$

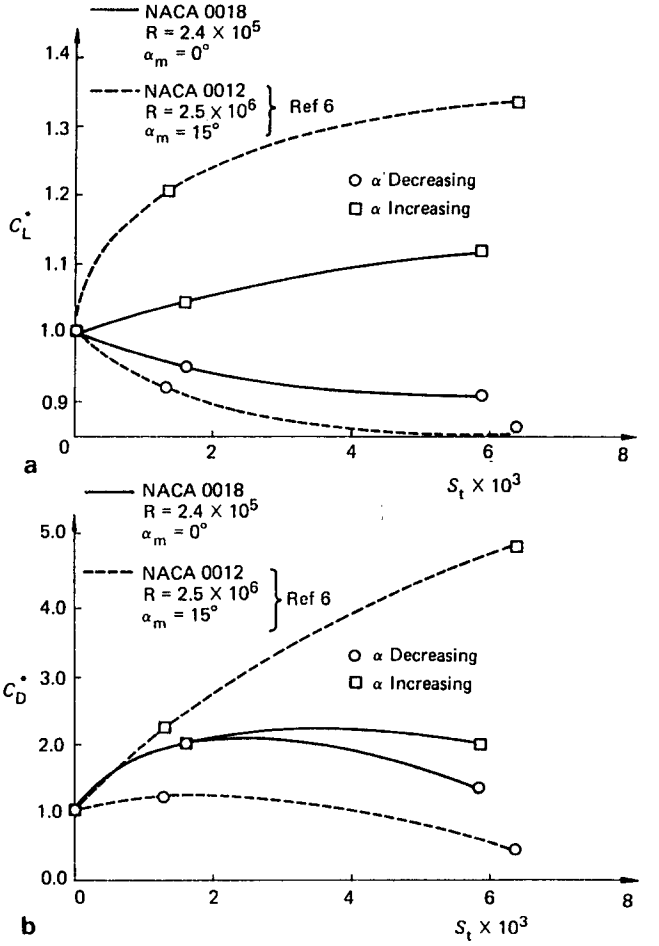

Fig 12 (a) Effect of reduced frequency on C_{Lmax}; (b) Effect of reduced frequency on C_{Dmax}

occurs for $\alpha = 14°$. The drag coefficients shown here are only for the pressure drag component. It is plausible that the skin friction drag could also vary with the reduced frequency.

The effect of reduced frequency on C_{Lmax} and the corresponding value of C_D is shown in Figs 12a and 12b. The results for C_L and C_D are dimensionless with respect to the corresponding values at $S_t = 0$. Also shown in the figure are the results obtained from Ref 6 for comparison. Although the two cases are not strictly comparable due to differences in the thicknesses of the aerofoils, Reynolds number and the mean incidence angle of oscillations, the trend of results appears to be similar. Both the results show that with the reduced frequency C_L and C_D increase with increasing incidence angle and decrease with decreasing incidence angle. If one assumes that a significant parameter is the mean indicence angle the results show that pitching an aerofoil at incidence angles close to that for stall produces greater changes in the flow around it compared with the case of pitching at zero incidence angle.

Conclusions

The effect of oscillating a thick aerofoil about a mean incidence angle of 0° is to produce an increase in the maximum life coefficient and to postpone stall. But these increases are smaller than those obtained by oscillating an aerofoil around the stall incidence angle.

Acknowledgement

The authors wish to acknowledge the financial support from the UK Department of Energy for these investigations.

References

1. **Raghunathan, S. and Tan, T. P.** Aerodynamic performance of Wells air turbine. *J. Energy, May–June 1983*, **7**(3), *226–230*
2. **Raghunathan, S. and Ombaka, O. O.** Effect of frequency of airflow on the performance of the Wells turbine. *Int. J. Heat and Fluid Flow, June 1985*, **6**(2), *127–132*
3. **McCroskey, W. J.** Prediction of unsteady separated flows on oscillating airflows. *AGARD-LS, 94, 1978*, Paper No. 12
4. **Mehta, V. B.** Dynamic stall of an oscillating airflow. *AGARD CP227, 1977*, Paper No. 23
5. **Widmayer, E., Jr., Clevenson, S. A. and Leedbetter, S. A.** Some measurements of aerodynamic forces and moments at subsonic speeds on a rectangular wing of aspect ratio two oscillating about mid-chord. *NACA TN 4240, May 1958*
6. **Moss, G. I. and Murdin, P. M.** Two dimensional low speed wind tunnel tests on the NACA 0012 section including measurements made during pitching oscillations at the stall. *RAE TR 68104, May 1968*
7. **Carr, L. W., McAlister, K. W. and McCroskey, W. J.** Analysis of the development of dynamic stall based on oscillating airfoil experiments. *NASA TN D-8382, January 1977*
8. **McAlister, K. W., Carr, L. W. and McCroskey, W. J.** Dynamic stall experiments on the NACA 0012 airfoil. *NASA TP 1100, January 1978*
9. **Windsor, R. I.** Measurements of aerodynamic forces on an oscillating airfoil. *Maryland Univ. College Park Dept. of Wind Tunnel OPER-ETC, USAAVLABS-TR-69-98, March 1970*
10. **Jacobs, E. N. and Sherman, A.** Airfoil section characteristics as affected by variation of the Reynolds number. *NACA Report No. 586, 1937*